



HAL
open science

Isostatic response of the lithosphere beneath the Mozambique Ridge (SW Indian Ocean) and geodynamic implications

Marcia Maia, M Diament, M Recq

► To cite this version:

Marcia Maia, M Diament, M Recq. Isostatic response of the lithosphere beneath the Mozambique Ridge (SW Indian Ocean) and geodynamic implications. *Geophysical Journal International*, 1989, 10.1111/j.1365-246X.1990.tb00689.x . insu-01354709

HAL Id: insu-01354709

<https://insu.hal.science/insu-01354709>

Submitted on 19 Aug 2016

HAL is a multi-disciplinary open access archive for the deposit and dissemination of scientific research documents, whether they are published or not. The documents may come from teaching and research institutions in France or abroad, or from public or private research centers.

L'archive ouverte pluridisciplinaire **HAL**, est destinée au dépôt et à la diffusion de documents scientifiques de niveau recherche, publiés ou non, émanant des établissements d'enseignement et de recherche français ou étrangers, des laboratoires publics ou privés.

Isostatic response of the lithosphere beneath the Mozambique Ridge (SW Indian Ocean) and geodynamic implications

M. Maia^{1,2,3}, M. Diament² and M. Recq¹

¹GEMCO (UA 718 du CNRS), Département de Géologie Dynamique, Université Paris VI, T.26-16, 4 Place Jussieu, 75252 Paris CEDEX 05, France

²Laboratoire de Géophysique (UA 730 du CNRS), Université de Paris-Sud Bât. 509, 91405 Orsay CEDEX, France

³CNPq, Av. W-3 Norte, Qd. 511, B1. A, Ed. Bittar II, 70750 Brasília, Brazil

Accepted 1989 August 10. Received 1989 August 10; in original form 1988 November 11

SUMMARY

The SW Indian Ocean is characterized by the presence of several aseismic features. The Mozambique Ridge, an elongated feature lying roughly parallel to the SE coast of Africa, is by far the least known of those structures, mainly due to the scarcity of marine data. To date, the crustal nature and the origin of the ridge are still controversial points. Since knowledge of the origin of the Mozambique Ridge is important for a better understanding of the evolution of the SW Indian Ocean, the isostatic response of the lithosphere beneath the ridge is analysed in order to characterize its effective elastic thickness and the emplacement process of the feature. Two different approaches are applied, the direct computation of the geoid anomaly over the ridge, by means of a 2.5-dimensional method, and the computation of the admittances between the bathymetry and both the geoid and gravity anomalies. Both approaches point to a local isostatic response of the lithosphere. The crustal thickness beneath the Mozambique Ridge ranges from 17 to 30 km and the average density, from 2.78 to $2.7 \times 10^3 \text{ kg m}^{-3}$, varying with locality, in good agreement with the few existing refraction profiles. Based on our results, on the geochemical similarity between the basalts cored at the DSDP site 249 and the MOR basalts (Erlank & Reid 1974; Thompson *et al.* 1982) and on the present knowledge of the SW Indian Ocean kinematics (Martin & Hartnady 1986), we propose an on-ridge origin for the Mozambique Ridge. The ridge would have been formed by the anomalous activity of a spreading axis linking the northern Mozambique and the Transkei basins accretion centres, between M10 and M2 times. At the M2 epoch, a ridge jump event would have caused the spreading to cease. The Astrid Ridge, a poorly known aseismic structure lying close to the coast of Antarctica near 15°E, may be the antarctic counterpart of the Mozambique Ridge, formed by the same accretionary phenomenon, the two ridges breaking apart at M2 time due to the ridge jump event. However, any admittance computation at such high latitudes is impossible at present, due to the very poor quality of both bathymetry and altimetry, and so this hypothesis cannot be verified.

Key words: altimetry, gravity data, isostatic response, lithosphere, Mozambique Ridge.

1 INTRODUCTION

Knowledge of the rheology of oceanic lithosphere has considerably improved during the last decade, allowing the use of observations of flexure to estimate the emplacement setting for plateaux and other oceanic features (e.g. Detrick

& Watts 1979; Bulot *et al.* 1984; Watts & Ribe 1984; Goslin *et al.* 1985; Deplus & Dubois 1986; Diament & Goslin 1986; Goslin & Diament 1987).

The deformation of the lithosphere when submitted to a load is mainly controlled by its effective elastic thickness, (EET). Several studies showed that the EET is directly

related to the age of the oceanic lithosphere at the time of loading (Watts & Cochran 1974; Bodine, Steckler & Watts 1981; McNutt & Menard 1982). It is thus possible, in most cases, to determine the approximate age of the lithosphere at the time of the emplacement of a feature by studying the isostatic response, i.e. the EET of the lithosphere beneath the load. An old, rigid lithosphere tends to deform regionally, while a young, thinner lithosphere, deforms locally. Such variations, reflecting differences in the strength of the lithosphere at the time of the load emplacement, can be used to discriminate between possible genetic processes, mainly whether related to an active spreading centre (low EET) or to intraplate phenomena (high EET). The relation of age to EET, however, can be locally altered by pronounced thermal effects (McNutt & Menard 1982; McNutt 1984). Heating reduces the strength of the lithosphere, its EET then being related to a thermal age rather than to that computed from magnetic anomalies (McNutt 1984). Such a thermal rejuvenation is mainly associated with features created by hotspot activity. Yet an on-ridge origin, i.e. related to spreading centre activity, can hardly be confounded with an off-ridge, intraplate origin. Hotspot thermal effects are probably not strong enough to reset the EET of the oceanic lithosphere down to very low values, characteristic of an on-ridge emplacement. Moreover, such thermal anomalies are typically associated either with topographic swells or with lineations of volcanic features, sometimes with both, generally allowing the detection of the passage of the oceanic lithosphere above a hotspot. However, attention has to be paid to structures created by major intraplate phenomena, since an underestimate of the EET of the lithosphere can lead to the suggestion of younger ages for their formation.

One of the most remarkable features of the SW Indian Ocean (Fig. 1) is the great number of aseismic structures found there (Goslin 1981). Characterization of the EET of the lithosphere beneath the Madagascar Plateau (Goslin *et al.* 1985), the Crozet Bank and Del Cano Rise (Goslin & Diament 1987), the Ob, Lena and Marion Dufresne seamounts (Diament & Goslin 1986) and the Kerguelen Plateau (Goslin & Diament 1987) led to the proposal of different ages and origins for these features, giving useful information concerning the evolution of that ocean.

The Mozambique Ridge (Figs 1 and 2) is one of the most poorly surveyed aseismic features of the Indian Ocean. At present, its nature, whether continental or oceanic, is not well constrained, mainly due to the scarcity of marine data. A few refraction profiles (Fig. 2) have been obtained in the oceanic basins of Transkei and Mozambique and also on the Mozambique Ridge (Ludwig *et al.* 1968; Hales & Nation 1973; Chetty & Green 1977). Of the profiles shot on the ridge, one reached the Moho discontinuity at a depth of 22.2 km beneath sea level (Hales & Nation 1973). Hales & Nation (1973) and Recq & Goslin (1981), using refraction results, proposed a local, Airy type, isostatic equilibrium for the Mozambique Ridge and the adjacent oceanic basins, with a crustal thickening of 15 km under the ridge and an average density of $2.81 \times 10^3 \text{ kg m}^{-3}$.

The DSDP site 249 (Fig. 2), located near the ridge crest, reached basalts of undetermined age, geochemically similar to those of the Mid Ocean Ridge (Erlank & Reid 1974; Thompson *et al.* 1982). Such an argument, without being

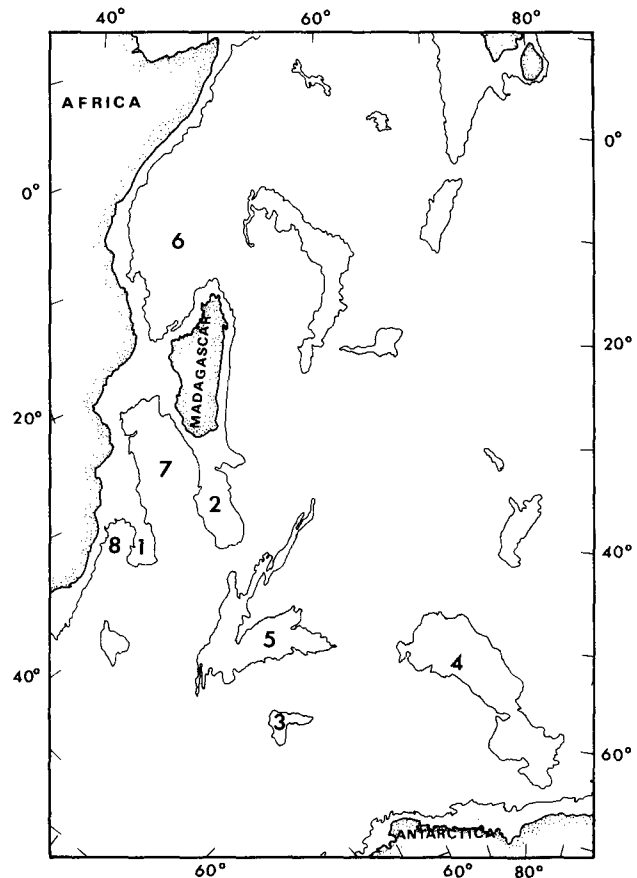


Figure 1. Main physiographic features of the SW Indian Ocean mentioned in the text. 1—Mozambique Ridge; 2—Madagascar Plateau; 3—Ob, Lena and Marion Dufresne Seamounts; 4—Kerguelen Plateau; 5—Del Cano Rise; 6—Somali Basin; 7—Mozambique Basin; 8—Transkei Basin. Oblique azimuthal equal area projection. Depth contour is 3000 m.

conclusive, favours an oceanic origin for the structure.

A thorough understanding of the nature and origin of the Mozambique Ridge is important to improve our understanding of the evolution of the SE continental margin of Africa and of the SW Indian Ocean as a whole. We present here an analysis of gravity and altimetric data, carried out in order to characterize its emplacement process by computing the EET of the lithosphere beneath the ridge.

2 GEODYNAMICAL SETTING

The Mozambique Ridge (Figs 1, 2, 3) is an elongated feature, lying roughly parallel to the coast of SE Africa between 25° and 35°S. It is bounded to the east by a 3000 m deep scarp, which descends into the Mozambique Basin and bears the same orientation as the fracture zone system parallel to the Prince Edward Fracture Zone. Both the abrupt topography and the direction of the scarp lead to the suggestion that there is a relation with the fracture zones that drove the southward movement of Antarctica during the later stages of the opening of the SW Indian Ocean. The eastern and the western flanks of the ridge are strikingly different, the later dropping with a gentle slope into the Transkei Basin, where sediment thicknesses probably reach 3 km (Hales & Nation 1973; Chetty & Green 1977).

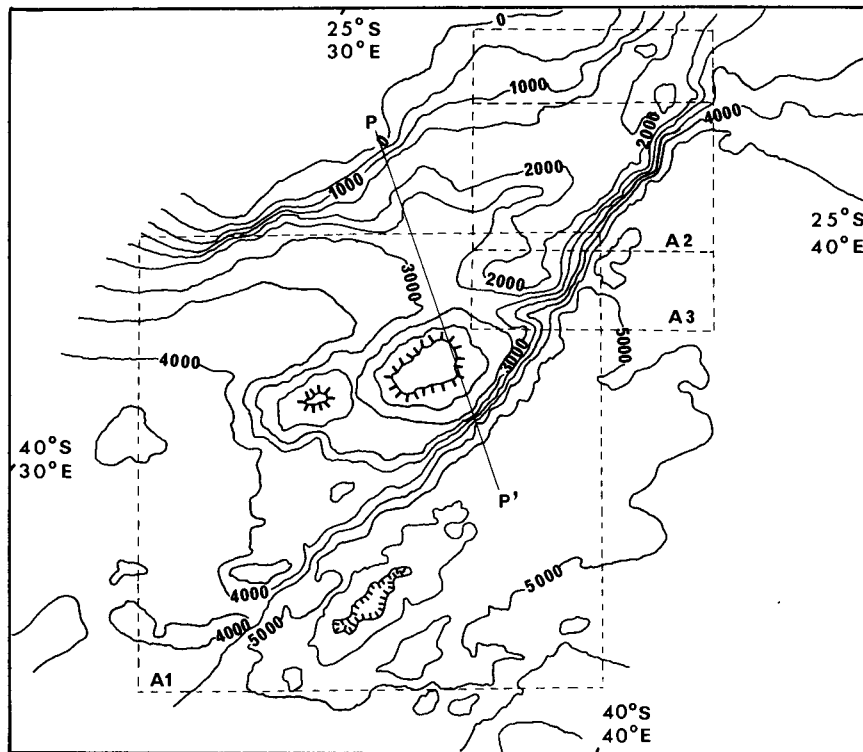


Figure 3. DBDB5 bathymetric map of the Mozambique Ridge between 25° and 40°S and 30° and 40°E, projected using the Lambert conical projection. Section P–P' shows the location of the SEASAT profile used for direct modelling. The boxes display the studied Areas 1, 2 and 3. Depth contour intervals are of 500 m.

admittance, between bathymetry and the potential field anomalies is now a usual approach in the analysis of the oceanic lithosphere rheology (e.g. Goslin *et al.* 1985; Diament 1987). Basically, we seek a linear filter which,

convolved with the bathymetry, is best able to reproduce the observed geoid or gravity anomaly.

The linear relation between gravity or altimetry and bathymetry, assuming a 3-D geometry, can be written as

$$g(x, y) = f(x, y) * b(x, y) + n(x, y) \quad (1)$$

where $n(x, y)$ is the noise, including the part of gravity or geoid not linearly related to bathymetry. In the spectral domain, this convolution becomes a simple multiplication

$$G(k) = Z(k)B(k) + N(k) \quad (2)$$

where $Z(k)$ is the admittance and $k = (kx^2 + ky^2)^{1/2}$ is the wavenumber, $2\pi/\lambda$, where λ is the wavelength.

Assuming that the geoid (or the gravity) is noisier than the bathymetry, an estimator of $Z(k)$ is given by (McKenzie & Bowin 1976)

$$Z(k) = \frac{\langle G(k)B^*(k) \rangle}{\langle B(k)B^*(k) \rangle} \quad (3)$$

where the symbol $*$ denotes the complex conjugate, $G(k)B^*(k)$ is the cross spectrum of the gravity or geoid and the bathymetry and $B(k)B^*(k)$ is the power spectrum of the bathymetry. The brackets denote the averaging in the spectral domain over a series of profiles in a 2-D case, or over a waveband annulus, in a 3-D case (McNutt 1979). The observed admittances are then compared with theoretical values derived from several models of isostatic response. The theoretical admittance for a plate model, considering the geoid anomaly, is given by (e.g. Banks, Parker &

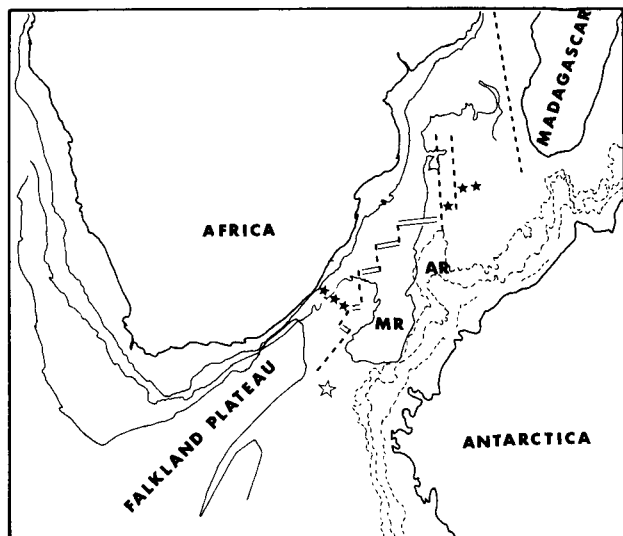


Figure 4. Schematic reconstruction for the M10 epoch from Martin & Hartnady (1986). Dashed lines locate the main fracture zones. Solid stars show the position of the active spreading centres in the Transkei and Mozambique Basins from M10 to M2 times and the double lines that of the hypothetical spreading axis between the two. The open star shows the location of the spreading centre at M2 times, after the ridge jump event. MR and AR denote the Mozambique and Astrid ridges, respectively.

Huestis 1977)

$$Z(k) = \frac{2\pi G}{gk} (\rho_c - \rho_w) \exp(-kd) \times \left[1 - \frac{g(\rho_m - \rho_c) \exp(-kT_c)}{(k^4)D + g(\rho_m - \rho_c)} \right] \quad (4)$$

where ρ_m , ρ_c and ρ_w are the densities of the upper mantle, crust and water respectively, and D is the flexural rigidity, given by:

$$D = E(T_c^3)/12(1 - \mu^2) \quad (5)$$

where T_c is the effective elastic thickness, E is the Young modulus and μ is the Poisson coefficient.

For a local Airy-type model, the theoretical expression of the admittance is obtained with $T_c = 0$:

$$Z(k) = \frac{2\pi G}{gk} (\rho_c - \rho_w) \exp(-kd)[1 - \exp(-kT_c)]. \quad (6)$$

The parameter T_c in the above equations gives the average depth of a major density contrast interface. In an Airy model, such an interface is usually assumed to be the crust-mantle boundary; T_c is therefore the average crustal thickness. For a thin elastic plate model, low T_c (such as 6 or 8 km) is interpreted as being the crustal thickness, these values being close to those of a normal oceanic crust. However, a high T_c and a high T_c are quite incompatible if the former is assumed to be the average crustal thickness. Goslin & Diament (1987) suggested that in such cases, T_c is better understood as being the average depth of an interface displaying a density contrast, caused by low-density material derived from a thermal or a chemical anomaly.

The best theoretical fit gives an approximation of the lithosphere rigidity. In practice, the best fit is obtained by varying T_c and T_c in a given range and minimizing the rms values. Usually, the average depth d and the crustal density ρ_c are set to reasonable values, or allowed to vary in a very narrow interval. Therefore, the main advantage of admittance computation is to characterize the isostatic response without any *a priori* assumptions.

A set of parameters is computed together with the observed admittances, in order to test their reliability. Among those, the most significant is the coherence, which is a measure of the part of the observed geoid or gravity directly attributed to bathymetry. An estimator of the coherence is given by:

$$Co(k) = \frac{\langle B(k)G^*(k) \rangle \langle B(k)G^*(k) \rangle}{\langle B(k)B^*(k) \rangle \langle G(k)G^*(k) \rangle}. \quad (7)$$

Munk & Cartwright (1966) observed that this estimator could be affected by the presence of noise in the data sets. They suggested computation of an unbiased estimate of the coherence by:

$$C(k) = [NCo(k) - 1]/(N - 1) \quad (8)$$

where N is the number of statistically independent observations in the considered waveband annulus.

We computed the coherence using both estimators. Since the computed values are only slightly different, we decided to retain the classical coherence definition.

The variance of the coherence estimator is given by (Bendat & Piersol 1986):

$$\text{Var}[Co(k)] = [2Co(k)][1 - Co(k)]^2/N. \quad (9)$$

Using the coherence estimator, we can compute the variance for the admittance estimator (Bendat & Piersol 1986):

$$\text{Var}[Z(k)] = \frac{[1 - Co(k)]Z^2(k)}{2Co(k)N}. \quad (10)$$

The normalized random error for the coherence estimate can be then computed (Bendat & Piersol 1986):

$$\text{Err}[Co(k)] = \frac{\text{Var}[Co(k)]^{1/2}}{Co(k)}. \quad (11)$$

Admittance values related to normalized random errors in the coherence larger than 0.25 were rejected, since this would imply the presence of non-Gaussian random noise in one or both data sets at the considered waveband. In such a case, both the admittance and the coherence will not obey normal distribution statistics and the computation of the estimates in a least-squares sense will be meaningless. We observed that the admittances and coherences associated with strong random errors are systematically biased to abnormally low values. Low coherences can either show that a significant portion of the energy in the observed geoid or gravity cannot be assigned to bathymetry, or that strong noise occurs on both data sets (Forsyth 1985; Dalloubeix, Fleitout & Diament 1988).

Here again, the choice between a 2- or a 3-D approach should be carefully considered. Applying a 2-D computation to a marked 3-D feature can lead to an overestimate of the effective elastic thickness (Ribe 1982). Also, the 3-D approach bears some advantages, such as allowing the possibility of studying an eventual anisotropy of the mechanical behaviour of the lithosphere (McNutt 1979). Here, we selected the second approach.

4 DATA AND DATA PROCESSING

We employed data from the world gridded bathymetry DBDB5, containing one point every 5' of latitude and longitude. The geoid was part of the global altimetric geoid derived from SEASAT data and interpolated every 0.25° (Marsh *et al.* 1986). Gravity was derived from the same altimetric data set at the Bureau Gravimétrique International (BGI), Toulouse (Balmino *et al.* 1987). Wavelengths longer than 4000 km were removed from both altimetry and gravity, using the global field model GRIM3L1 (Reigber *et al.* 1985). No corrections for age variations or sediment thicknesses were applied, due both to the small size of the zone and to the lack of reliable seismic data.

The gridded data were projected using a Lambert conical projection and interpolated with a spline bicubic function and a 30-km step. The step (larger than the original one of the data files) was chosen since it was believed that, due to the small amount of marine data in the area, the DBDB5 original step is unreliable. The final bathymetric, altimetric and gravimetric maps are displayed on Figs 3, 5 and 6.

Two slightly different topographic domains are noticeable (Fig. 3). The southern domain has a rough circular form,

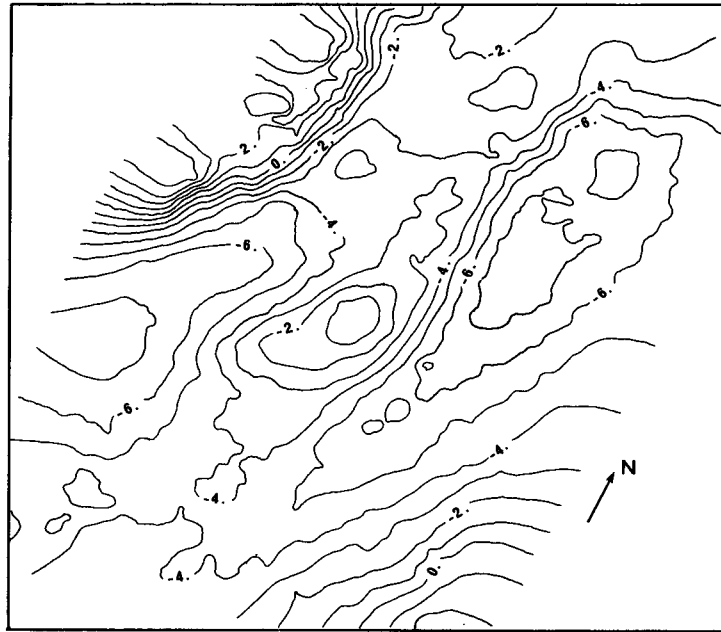


Figure 5. Altimetric geoid over the Mozambique Ridge, from gridded world geoid of Marsh *et al.* 1986. Contour interval is 1 m.

reaching depths of less than 1500 m. The northern domain has a smoother topography and a more elongated shape, passing gradually to the north into the Mozambique Channel. As no seismic data are available for the northern part of the ridge, it was not possible to determine whether the topographic differences arise from structural changes or from a thicker sedimentary covering to the north.

The altimetric geoid map (Fig. 5) displays an elongated anomaly over the ridge, well correlated with the bathymetry. The eastern scarp signature is clearly outlined, while the anomaly over the western flank reflects the gentle transition into the Transkei Basin. Differences between southern and northern parts of the ridge are smoothed,

although the southern domain displays a slightly higher anomaly, roughly following the bathymetric contours.

Free-air anomalies (Fig. 6) are not large, the average difference between the ridge and the oceanic basins being 40 mgal. The ridge itself appears as a 20 mgal relative high, and up to 60 mgal on its southern part.

Three square areas were selected for the analysis (Fig. 3). The first, with a 930-km side, comprises the southern domain, while the two others, each with a 450-km side, are centred over the northern plateau and scarp. Those areas were selected in an attempt to determine eventual different isostatic responses between the northern and the southern parts of the ridge.

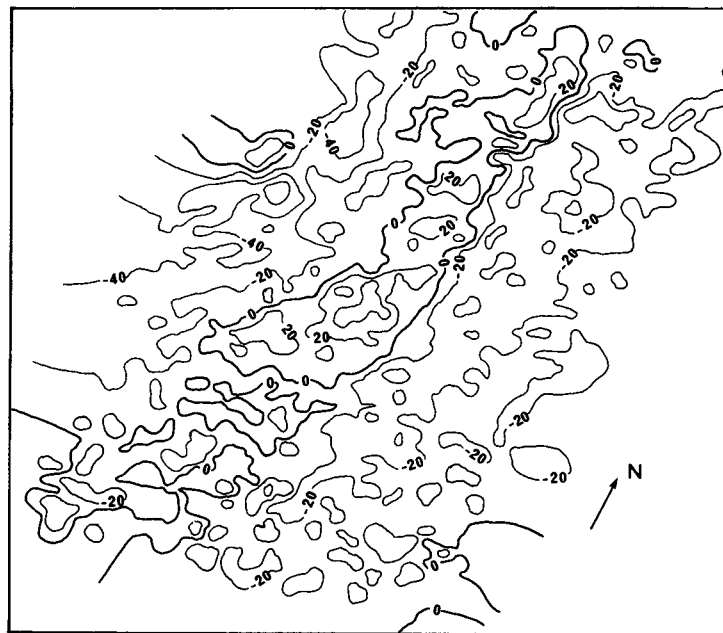


Figure 6. Altimetric derived free-air anomalies over the Mozambique Ridge. Contour interval is 20 mgal.

Two different treatments to minimize edge effects were applied to the gridded data, in order to check the computation stability: tapering with a cosine window and mirror imaging. On applying the cosine window, the linear trend related to the continental margin was removed by fitting a plane to the gridded data in order to reduce the edge effects, though such a procedure may introduce errors in the longest wavelength, biasing the admittance to a lower value (Diament 1985). Mirror imaging does not require the removal of a linear trend from the data. However, attention should be paid to the admittance values used in the determination of the best fitting model, as only those corresponding to the original length of the studied area should be considered (Diament 1985).

Descending altimetric SEASAT profiles (Fig. 3) were used for the direct modelling. Wavelengths longer than 4000 km were removed, together with the linear trend. The profiles were projected orthogonally to the ridge axis, as required by the 2.5-dimensional method. Note, however, that the projection angle is very small, since the ridge is nearly normal to the descending SEASAT profiles.

5 RESULTS AND DISCUSSION

5.1 Direct modelling

The crustal model used to compute the geoid anomaly was constructed from the available seismic profiles (Hales & Nation 1973; Chetty & Green 1977) and the GEBCO bathymetric map. The observed and the computed anomalies are displayed in Fig. 7. The poor quality of both bathymetry and seismics prevents the development of a detailed model and we could not obtain a higher quality fit. Nevertheless, the peak and the general form of the observed anomaly are reasonably matched by an anomaly created by a local isostatic response model, assuming a 25 km deep crustal root with density $2.8 \times 10^3 \text{ kg m}^{-3}$ under the ridge.

5.2 Admittance computation

The mirror imaging and the cosine window taper plus trend removal techniques were applied to altimetric data from

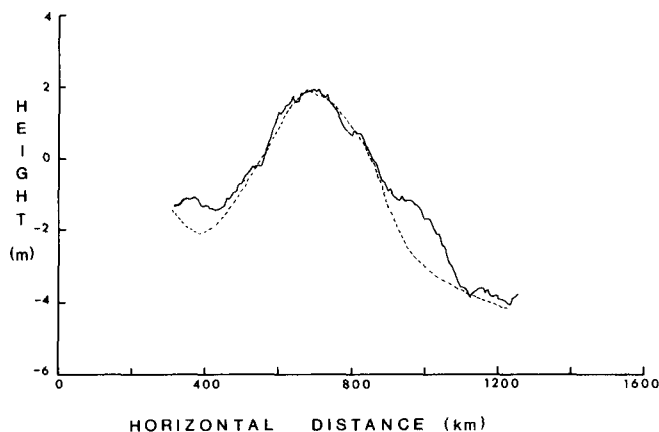


Figure 7. Computed and observed geoid anomalies across the Mozambique Ridge. The location of the SEASAT profile is shown in Fig. 3.

Area 1 (Fig. 8a,b). Both yielded close results, the latter, as expected, slightly biasing the first computed admittance to a lower value. The scatter is lower for the admittances computed using the mirror imaging and the quality of the theoretical fit is also better. The coherence values (Figs 9a,c) also agree well, and the normalized random errors (Fig. 10a,c) at the longer wavelengths are higher for the cosine tapered data. Therefore, we decided to apply the mirror imaging technique to all three boxes.

The comparison between the gravity and the altimetry was also only performed for Area 1. Both data sets were processed using the mirror imaging technique. The computed admittances are displayed in Fig. 8(a,c), the coherences in Fig. 9(a,b) and the normalized random errors in Fig. 10(a,b). The coherences are high only for wavelengths longer than 186 km for both altimetry and gravity. So, in this area, gravity deduced from altimetry does not improve the quality of the admittance computations for the shorter wavelengths, possibly due to noise in the DBDB5 bathymetry. The scatter of the computer admittances is higher for the gravity data than for the altimetric data. The gravimetric admittance shows a very flat behaviour and the theoretical fit is of rather poor quality. Normalized random errors for the longer wavelengths are smaller for the altimetric coherences, with the exception of the point at the 230-km wavelength. At this point both the admittances and the coherences computed for Area 1 are biased to low values, the effect being stronger for the altimetric admittances. These anomalous values are probably related to the presence of noise in both data sets at the considered wavelength (Dalloubeix, Fleitout & Diament 1988).

The computed altimetric admittances for Areas 1, 2 and 3 are displayed on Fig. 8(a,d,e), together with the corresponding theoretical fit, achieved by varying T_e , T_c , ρ_c and d simultaneously. The rms for the best fits are shown in Fig. 11(a, e and f). The fit parameters are shown in Table 1. The best fit was always obtained for a local isostatic response, $T_e = 0$ km. The crustal thickness, T_c , is higher for the southern area (30 km) than for the northern areas (20 and 16 km), reflecting the higher topography. Although the density is also slightly higher for Area 1 ($2.78 \times 10^3 \text{ kg m}^{-3}$) than for Areas 2 and 3 (2.7×10^3 and $2.74 \times 10^3 \text{ kg m}^{-3}$), such small variations would produce quite similar theoretical curves with slight differences in the crustal thicknesses, without significant implications for the fit. Fig. 11(a,b and c) shows best fits for Area 1 obtained with different densities. The crustal thickness is only slightly higher (2 km) for a density of 2.7×10^3 (Fig. 11c). Therefore, we do not regard the density variation as significant. The average density values are higher than those obtained with the same technique for other aseismic features of the Indian Ocean, e.g. $2.6 \times 10^3 \text{ kg m}^{-3}$ for the southern Madagascar Plateau (Goslin *et al.* 1985) and the Del Cano Rise (Goslin & Diament 1987) and are typical of an oceanic domain.

No azimuthal trend is visible in the residual geoid anomalies, allowing us to suppose that no significant anisotropy in the mechanical rheology of the lithosphere exists in the studied area (McNutt 1979).

Our results, which show that the Mozambique Ridge is locally compensated, corroborate the hypothesis suggested by Recq & Goslin (1981), of an Airy type isostatic

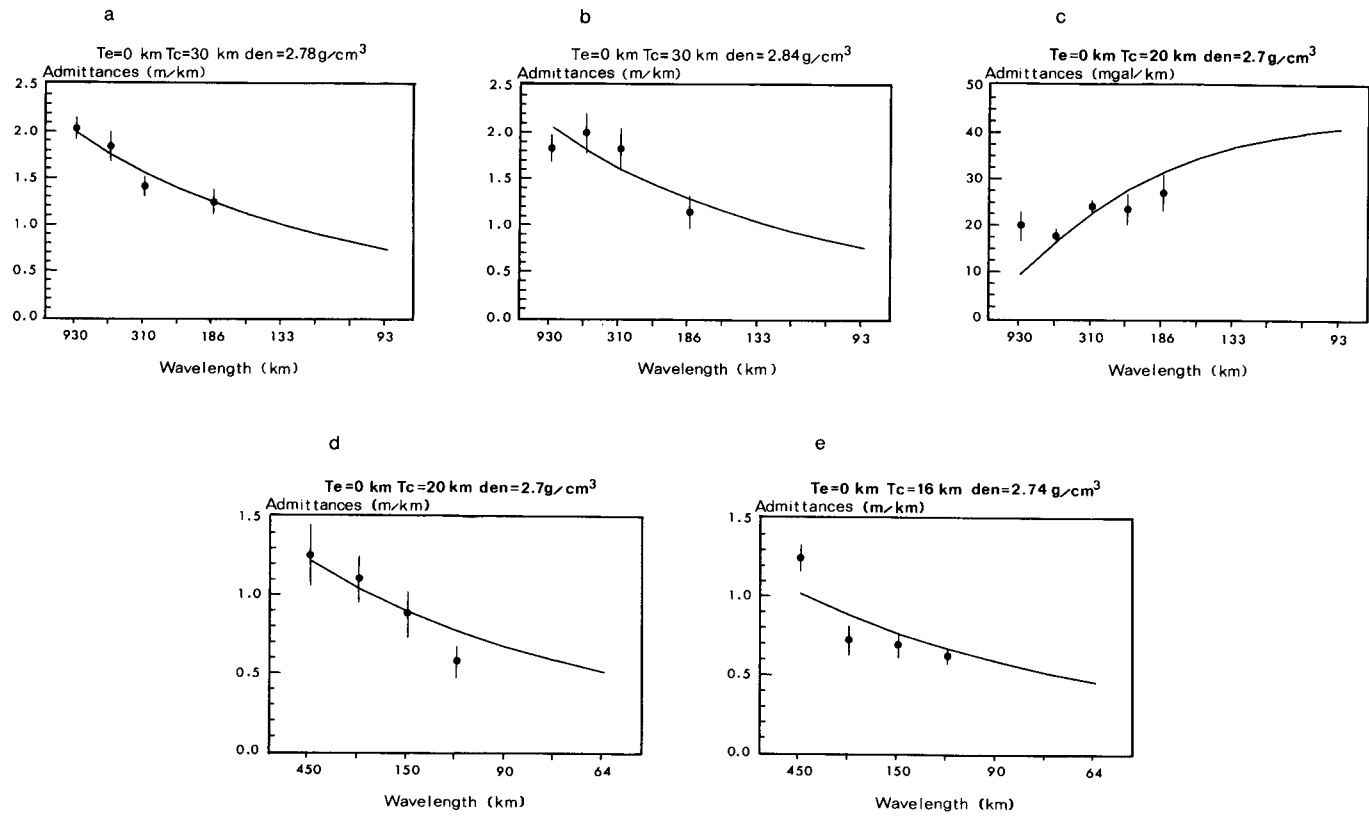


Figure 8. Computed and theoretical admittances. (a) Altimetric admittances for Area 1, mirror imaging. (b) Altimetric admittances for Area 1, cosine window taper plus trend removal. (c) Gravimetric admittances for Area 1, mirror imaging. (d) Altimetric admittances for Area 2, mirror imaging. (e) Altimetric admittances for Area 3, mirror imaging.

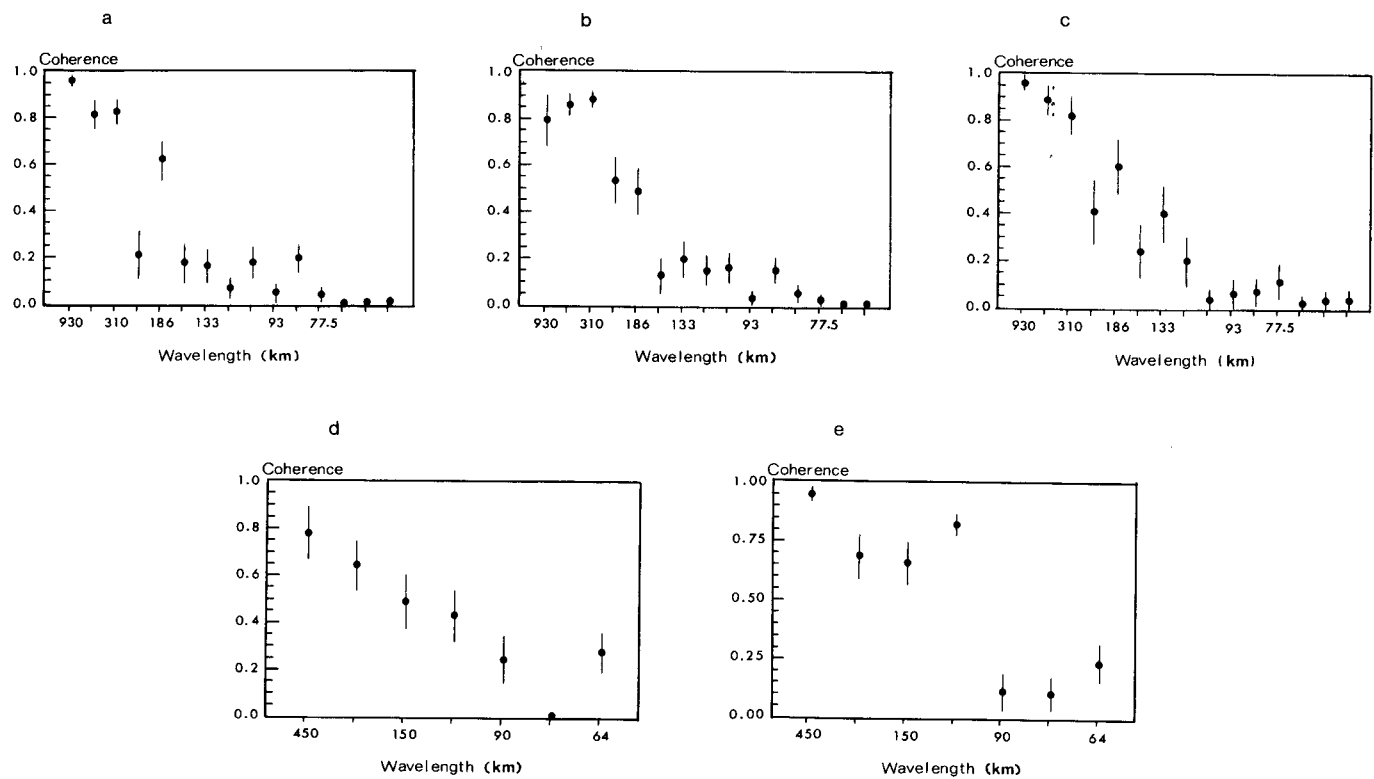


Figure 9. Coherence functions. (a) Area 1, altimetric data and mirror imaging. (b) Area 1, gravimetric data and mirror imaging. (c) Area 1, altimetric data and cosine window taper. (d) Area 2, altimetric data and mirror imaging. (e) Area 3, altimetric data and mirror imaging.

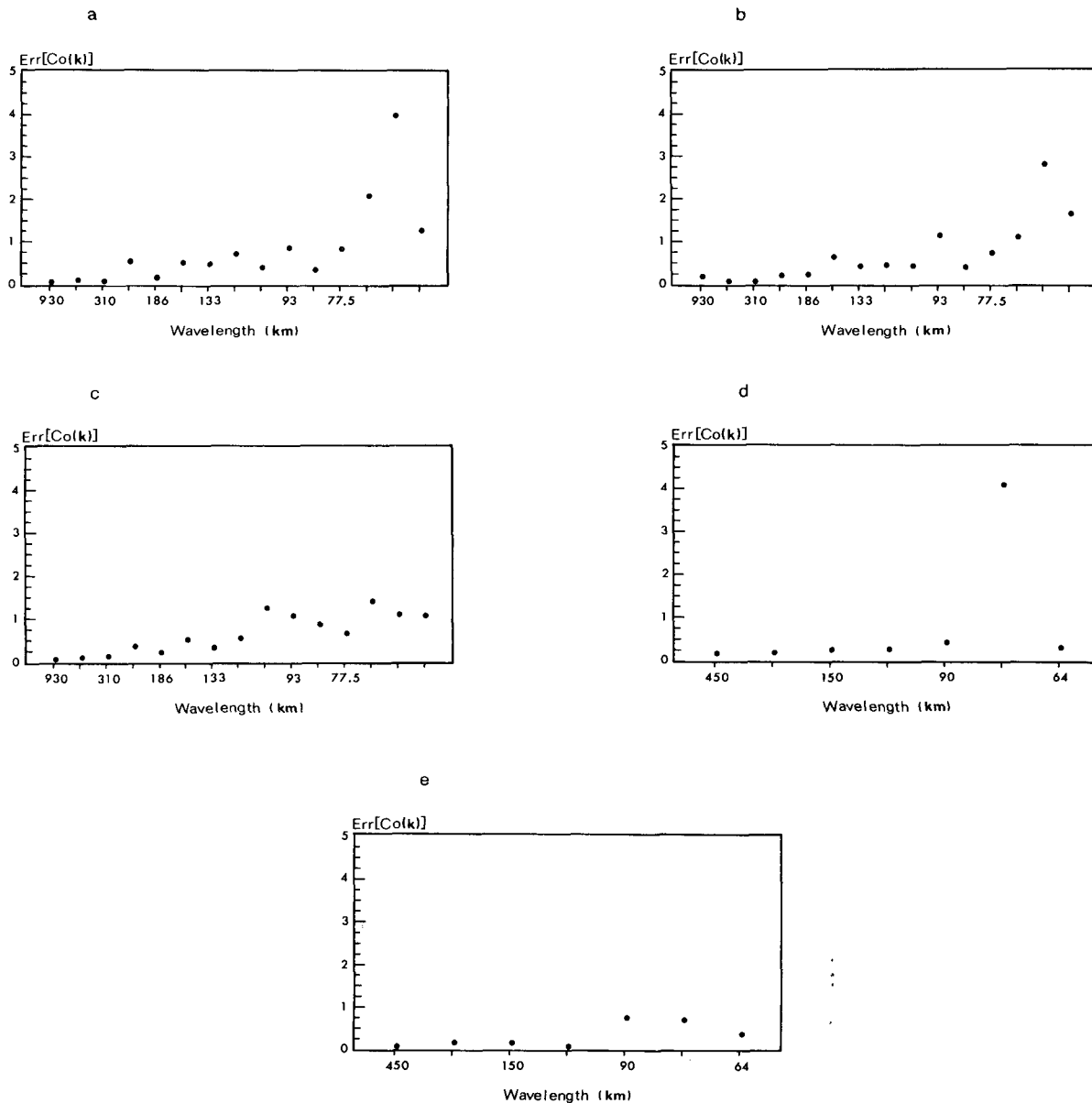


Figure 10. Normalized random errors for the coherences. (a) Area 1, altimetric data and mirror imaging. (b) Area 1, gravity data and mirror imaging. (c) Area 1, altimetric data and cosine window taper. (d) Area 2, altimetric data and mirror imaging. (e) Area 3, altimetric data and mirror imaging.

equilibrium between the ridge and the adjacent oceanic basins. Also, the geochemical analysis of the basalts drilled at the DSDP 249, similar to those of the Mid Ocean Ridge (Erlank & Reid 1974; Thompson *et al.* 1982), as well as the rather high average density values obtained in this study, seems to support an oceanic nature for the ridge. We consider the continental nature hypothesis very unlikely, although from our results, the possibility of a deeply altered continental crust, injected by oceanic basalts, cannot be totally discarded. However, a northernmost position for the Mozambique Ridge, as suggested by Martin & Hartnady (1986), seems improbable either for an oceanic or for an altered continental crust. It would imply an overlapping between the ridge and the southern Mozambique Channel, which is probably formed by thinned continental crust (Recq 1982). Therefore, we propose an oceanic on-ridge origin for

the Mozambique Ridge. The ridge would have been formed between M10 and M2 times, by the anomalous activity of a spreading axis running from the northern Mozambique to the Transkei basins accretion centres. This would imply the existence of a triple junction in the Transkei Basin, as proposed earlier by Martin & Hartnady (1986). Such an emplacement process avoids the necessity of a northern position for the Mozambique Ridge prior to M10 times. Its southern domain, which overlaps with Antarctica on pre-M10 refits (Martin & Hartnady 1986), was formed later, by the continuous activity of the spreading centre, while Antarctica drifted southwards (Fig. 4).

It is interesting to notice that the Astrid Ridge, Antarctica, juxtaposes the Mozambique Ridge at the M10 refit proposed by Martin & Hartnady (1986). Both ridges could have originally been a single structure, as they

suggested, created by the same accretionary phenomenon. At M2–M0 times, a spreading reorganization caused the Transkei Basin triple junction to migrate southwards. Also, the spreading direction in the Mozambique Basin changed, as Madagascar and Antarctica drifted apart. As a consequence, the Mozambique and Astrid ridges broke

apart, the first being left entirely on the African plate, the latter moving southwards attached to Antarctica (Martin & Hartnady 1986).

An analysis of the isostatic response beneath the Astrid Ridge would be interesting. However, the poor quality of both bathymetry and altimetry at high latitudes prevents, at

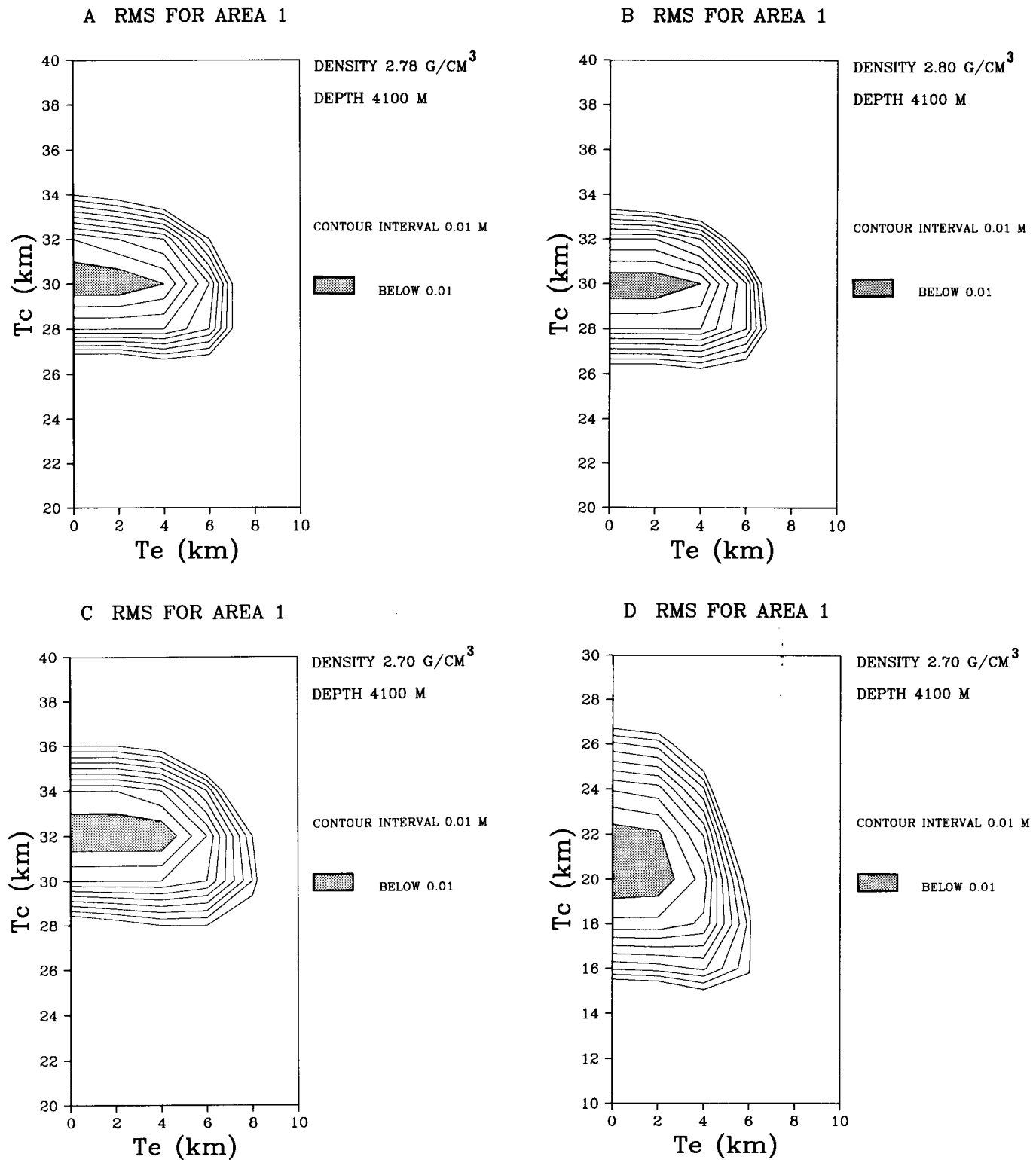


Figure 11. The rms errors for the theoretical fits. A, B and C: Area 1, altimetric data and mirror imaging. D: Area 1, gravity data and mirror imaging. E: Area 2, altimetric data and mirror imaging. F: Area 3, altimetric data and mirror imaging.

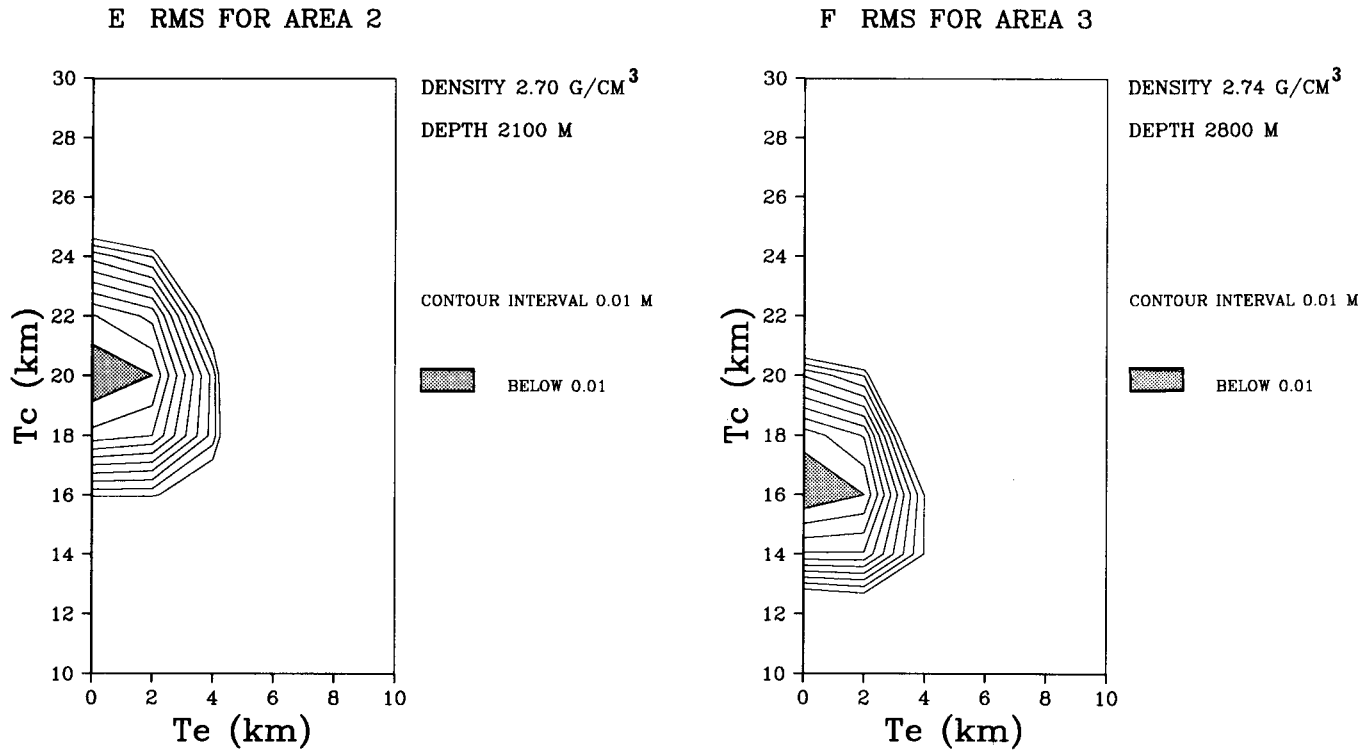


Figure 11. (continued)

Table 1. Best fit parameters for the computed altimetric admittances for Areas 1, 2 and 3.

| Area n° | Best fit parameters Tc, ρ_c , d, Te = 0 km | Data processing | Data |
|---------|---|---|-----------|
| 1 | Tc = 30 km ρ_c = 2.78 g/cm ³ d = 4100 m | Mirror imaging | Altimetry |
| 1 | Tc = 30 km ρ_c = 2.84 g/cm ³ d = 4100 m | Cosine window taper Trend removal | Altimetry |
| 1 | Tc = 20 km ρ_c = 2.70 g/cm ³ d = 4100 m | Mirror imaging | Gravity |
| 2 | Tc = 20 km ρ_c = 2.7 g/cm ³ d = 2100 m | Mirror imaging | Altimetry |
| 3 | Tc = 16 km ρ_c = 2.74 g/cm ³ d = 2800 m | Mirror imaging | Altimetry |

least at present, any computation of the admittance in those areas.

6 CONCLUSIONS

The local isostatic response of the lithosphere beneath the Mozambique Ridge suggests an on-ridge environment for its emplacement, assuming the ridge to be oceanic. The geochemical analysis of the DSDP site 249 basalts seems to support this hypothesis. The ridge, probably together with its antarctic counterpart, the Astrid Ridge, was formed between M10 and M2 times by anomalous activity of the

spreading centre, then active in the area. Such an anomalous activity is comprehensible, for the SW Indian Ocean spreading history is marked by a complex interaction of ridge jumps, triple junctions and spreading reorganizations (Goslin & Patriat 1984; Martin & Hartnady 1986).

ACKNOWLEDGMENTS

This work was carried out at the Laboratoire de Géophysique, Université de Paris Sud and partially funded by ATP-INSU 'Téledetection spatiale'. One of the authors (M.M.) was supported by a scholarship from the

IOC-UNESCO and from the CNPq, Brazilian Government. The authors are grateful to Yves Albouy (ORSTOM-Bondy, France) and to Dr Martin Sinha of Bullard Laboratories, University of Cambridge, for comments and improvements to the text. This is GEMCO contribution No. 490.

REFERENCES

- Balmino, G., Moynot, B., Sarrailh, M. & Valés, N., 1987. Free-air gravity anomalies over the oceans from SEASAT and GEOS 3 altimeter data, *EOS, Trans. Am. Geophys. Un.*, **68**, 17–19.
- Banks, R. J., Parker, R. L. & Huestis, S. P., 1977. Isostatic compensation on a continental scale: local versus regional mechanisms, *Geophys. J. R. astr. Soc.*, **51**, 431–452.
- Bendat, J. S. & Piersol, A. G., 1986. *Random Data: Analysis and Measurement Procedures*, John Wiley, New York.
- Bergh, H. W., 1977. Mesozoic seafloor off Dronning Maud Land, Antarctica, *Nature*, **269**, 686–687.
- Bodine, J. H., Steckler, M. S. & Watts, A. B., 1981. Observations of flexure and the rheology of the oceanic lithosphere, *J. geophys. Res.*, **86**, 3695–3707.
- Bulot, A., Diament, M., Kogan, M. G. & Dubois, J., 1984. Isostasy of aseismic tectonic units in the South Atlantic Ocean and geodynamic implications, *Earth planet. Sci. Lett.*, **70**, 346–354.
- Chapman, M. E., 1979. Techniques for interpretation of geoid anomalies, *J. geophys. Res.*, **84**, 3793–3801.
- Chetty, P. & Green, R. W. E., 1977. Seismic observations in the Transkei basin and adjacent areas, *Mar. geophys. Res.*, **3**, 197–208.
- Dalloubeix, C., Fleitout, L. & Diament, M., 1988. A new analysis of gravity and topography data over the Mid-Atlantic Ridge: non-compensation of the axial valley, *Earth planet. Sci. Lett.*, **88**, 308–320.
- Deplus, C. & Dubois, J., 1986. Etude gravimétrique et magnétique du mont sous-marin Erimo: résultats de la campagne Kaiko, *C. R. Acad. Sci. Paris*, **302**, 1155–1157.
- Detrick, R. S. & Watts, A. B., 1979. An analysis of isostasy in the world's oceans; 3 aseismic ridges, *J. geophys. Res.*, **84**, 3637–3653.
- Diament, M., 1985. Influence of method of data analysis on admittance computation, *Ann. Geophys.*, **3**, 785–792.
- Diament, M., 1987. Isostasie, reponses mécanique et thermique de la lithosphère. Applications à la géodynamique, *Thèse d'état*, Université de Paris-Sud, Paris.
- Diament, M. & Goslin, J., 1986. Emplacement of the Marion Dufresne, Lena and Ob seamounts (South Indian Ocean) from a study of isostasy, *Tectonophysics*, **121**, 253–262.
- Erlank, A. J. & Reid, D. L., 1974. Geochemistry, mineralogy and petrology of basalts, leg 25 Deep Sea Drilling project, *Init. Rep. Deep Sea Drill. Proj.*, **25**, 543–551.
- Forsyth, D. W., 1985. Subsurface loading and estimates of the flexural rigidity of continental lithosphere, *J. geophys. Res.*, **90**, 12 623–12 632.
- Goodlad, S. W., Martin, A. K. & Hartnady, C. J. H., 1982. Mesozoic magnetic anomalies in the southern Natal Valley, *Nature*, **295**, 686–688.
- Goslin, J., 1981. Etude géophysique des reliefs asismiques de l'Océan Indien occidental et austral, *Thèse d'état*, Université Louis-Pasteur, Strasbourg.
- Goslin, J. & Patriat, P., 1984. Absolute and relative plate motions and hypotheses on the origin of five aseismic ridges in the Indian Ocean, *Tectonophysics*, **101**, 221–244.
- Goslin, J. & Diament, M., 1987. Mechanical and thermal isostatic response of the Del Cano Rise and Crozet Bank (Southern Indian Ocean) from altimetry data, *Earth planet. Sci. Lett.*, **84**, 285–294.
- Goslin, J., Diament, M., Bulot, A. & Stephan, M., 1985. Réponse isostatique de la lithosphère dans la région du plateau de Madagascar (Océan Indien occidental), *Bull. Soc. geol. France*, **8**, 199–206.
- Hales, A. L. & Nation, J. B., 1973. A seismic refraction study in the Southern Indian Ocean, *Bull. seism. Soc. Am.*, **63**, 1951–1966.
- Kogan, M. G., Diament, M., Bulot, A. & Balmino, G., 1985. Thermal isostasy in the South Atlantic Ocean from geoid anomalies, *Earth planet. Sci. Lett.*, **74**, 280–290.
- Ludwig, W. J., Nafe, J. E., Simpson, E. S. W. & Sacks, S., 1968. Seismic refraction measurements on the Southeast African continental margin, *J. geophys. Res.*, **73**, 3707–3719.
- Marsh, J. G., Brenner, A. C., Beckley, B. D. & Martin, T. V., 1986. Global mean sea surface based upon the SEASAT altimeter data, *J. geophys. Res.*, **91**, 3501–3506.
- Martin, A. K. & Hartnady, C. J. H., 1986. Plate tectonics development of the South West Indian Ocean: a revised reconstruction of East Antarctica and Africa, *J. geophys. Res.*, **91**, 4767–4786.
- McKenzie, D. & Bowin, C. D., 1976. The relationship between bathymetry and gravity in the Atlantic Ocean, *J. geophys. Res.*, **81**, 1903–1915.
- McNutt, M. K., 1979. Compensation of oceanic topography: an application of the response function technique to the SURVEYOR area, *J. geophys. Res.*, **84**, 7589–7598.
- McNutt, M. K., 1984. Lithospheric flexure and thermal anomalies, *J. geophys. Res.*, **89**, 11 180–11 194.
- McNutt, M. & Menard, H. W., 1982. Constraints on yield strength in the oceanic lithosphere derived from observations of flexure, *Geophys. J. R. astr. Soc.*, **71**, 363–394.
- Munk, W. H. & Cartwright, D. E., 1966. Tidal spectroscopy and prediction, *Phil. Trans. R. Soc. Lond.*, **A 259**, 533–581.
- Parson, L. M., Roberts, D. G. & Miles, P. R., 1981. Magnetic anomalies in the Somali Basin, N.W. Indian Ocean, *Geophys. J. R. astr. Soc.*, **65**, 260–270.
- Rabinowitz, P. D., Coffin, M. F. & Falvey, F., 1983. The separation of Madagascar and Africa, *Science*, **220**, 67–69.
- Recq, M., 1982. Anomalies de propagation des ondes P à l'Est de la Ride de Davie, *Tectonophysics*, **82**, 189–206.
- Recq, M. & Goslin, J., 1981. Etude de l'équilibre isostatique dans le sud-ouest de l'Océan Indien à l'aide des résultats de réfraction sismique, *Mar. Geol.*, **41**, M1–M10.
- Reigber, C., Balmino, G., Müller, H., Bosch, W. & Moynot, B., 1985. GRIM gravity model improvement using LAGEOS (GRIM3-L1), *J. geophys. Res.*, **90**, 9285–9299.
- Ribe, N. M., 1982. On the interpretation of frequency response functions for oceanic gravity and bathymetry, *Geophys. J. R. astr. Soc.*, **70**, 273–294.
- Ségoufin, J., 1978. Anomalies magnétiques mésozoïques dans le bassin du Mozambique, *C.R. Hebd. Séances Acad. Sci.*, **287**, 109–112.
- Ségoufin, J. & Patriat, P., 1980. Existence d'anomalies mésozoïques dans le bassin de Somalie: implications pour les relations Afrique–Antarctique–Madagascar, *C.R. Hebd. Séances Acad. Sci.*, **291**, 85–88.
- Simpson, E. S. W., Sclater, J. G., Parsons, P., Norton, I. O. & Meinke, L., 1979. Mesozoic magnetic lineations in the Mozambique Basin, *Earth planet. Sci. Lett.*, **43**, 260–264.
- Thompson, G., Bryan, W. B., Frey, F. A., Dickey, J. S. & Davies, H., 1982. Petrology, geochemistry and original tectonic setting of basalts from the Mozambique Basin and Ridge (DSDP sites 248, 249 & 250) and from the southwest Indian Ridge (DSDP site 251), *Mar. Geol.*, **48**, 175–195.
- Watts, A. B. & Cochran, J. R., 1974. Gravity anomalies and flexure of the lithosphere along the Hawaiian-Emperor seamount chain, *Geophys. J. R. astr. Soc.*, **38**, 119–141.
- Watts, A. B. & Ribe, N. M., 1984. On geoid heights and flexure of the lithosphere at seamounts, *J. geophys. Res.*, **89**, 11 152–11 170.